Asymmetric Double Tetragonal Domain Packing from ABC Triblock Terpolymer Blends with Chain Length Difference

Yusuke Asai, Atsushi Takano, Yushu Matsushita*

Department of Applied Chemistry, Graduate School of Engineering, Nagoya University,

Furo-cho, Chikusa-ku, Nagoya 464-8603, Japan

E-mail: yushu@apchem.nagoya-u.ac.jp

Abstract

A specific phase structure was observed for binary blends of poly(isoprene)-*block*-poly(styrene)-*block*-poly(2-vinyl pyridine) (ISP) triblock terpolymers with asymmetric chain lengths of two end-blocks. Tetragonal-packed cylinders were obtained from various binary blends on a wide range of volume fractions, although the sizes of I and P cylinders were highly asymmetric. Those structures have never been found for monodisperse ABC triblock terpolymers, and the three specific features have been confirmed. They are 1) I cylinders were metamorphosed into rod domains, their interfaces have non-constant mean curvatures, 2) the cross-sectional area ratio of I /P domain is qualitatively changed with the volume fraction of each component and 3) spherical and cylindrical domains of P component coexist. The molecular design adopted in the present work, that is, I and P blocks in two parent terpolymers have both fairly large chain length difference, must lead to these new morphologies.

Introduction

Block copolymers composed of two or more chemically different components, spontaneously self-assemble into ordered microstructures in bulk.[1-3] The ability of self-assembled structures to exhibit a wide variety of morphologies and tunability of feature sizes has been fascinating researchers, and hence a large number of studies have been conducted both experimentally and theoretically.[4-7]

For the simplest block copolymer, AB diblock copolymer, it is well known that four classical structures, alternative lamellae, bicontinuous double gyroid, hexagonal-packed cylinders and bcc spheres, are typically created.[8-11] The phase behavior of AB diblock copolymers depends primarily on the degree of polymerization (N), the Flory-Huggins interaction parameter (χ_{AB}) and the volume fractions occupied by two components in a molecule (φ_A, φ_B).

The addition of a third component to produce ABC triblock terpolymers can provide morphological variety and complexity because the number of parameters such as three interaction parameters (χ_{AB}, χ_{BC}, χ_{AC}), volume fractions (φ_A, φ_B, φ_C,) and block sequences (ABC, ACB, BAC) increase. [2,3,12-22] The bridging of the central chains between the end blocks also leads to variety and complexity. For example, non-frustrated ABC triblock terpolymers with interaction parameters $\chi_{AB} \cong \chi_{BC} < \chi_{AC}$, show a phase diagram similar to those of AB diblock copolymers at equal volume fraction of A and C, $\varphi_A = \varphi_C$, in which three-phase four-layer lamellae, tricontinuous double gyroid, coarrayed

tetragonal-packed cylinders and spheres with a CsCl-type lattice are formed depending on φ_B. [3,12,13] When the interaction parameter between the two end blocks, $\chi_{AC,}$ is smaller than χ_{AB} or χ_{BC}, complex morphologies are obtained to construct structures with A/C interfaces since those molecules must be in a frustrated circumstance. Breiner and Liu have demonstrated that the frustrated systems have more complex morphologies than the non-frustrated ones. [17,22]

Although there are a lot of experimental and simulation results, a full understanding of the phase behavior of ABC triblock terpolymers has not been realized yet since triangle phase diagram must be considered. Especially in experiments, it is hard to cover the entire phase diagrams because a large number of ABC triblock terpolymers must be required to fill the diagram. To accomplish above difficulty, mixing of polymers is an efficient method to tune composition of block terpolymers without preparing new terpolymers. There are basically two ways; one is blending small molecular weight homopolymer(s) with ABC triblock terpolymers, the other is mixing ABC triblock terpolymers with block copolymers or terpolymers having two or three constituent blocks.

Blending the constituent homopolymers with ABC triblock terpolymers is a well-established technique for controlling morphology. [23-26] Note in some cases that triblock terpolymer/ homopolymer blend systems have proven to stabilize new ordered morphologies which are rarely found in neat triblock terpolymers, such as an orthorhombic network structure [23] and a cylindrical structure with a 5-coordinated packing.[26] Dotera presented numerical evidence of the creation of tricontinuous double

diamond and also double primitive structures in ABC/A/C blends, using the Monte Carlo lattice-simulation technique.[27]

Blends of ABC triblock terpolymers and block copolymers have also attracted many researchers because the phase diagram of block copolymer blends is significantly different from that of block terpolymer/ homopolymer blends.[28-35] In contrast to block terpolymer/ homopolymer blend systems, where the stable structure depends on the molecular weight ratio of the homopolymer and the corresponding block, the chemical junctions of the blended polymers have to share a common interface of microdomains, resulting in characteristic morphological behavior such as core-shell type superlattices and non-centrosymmetric superlattice. [28-31] Furthermore, a large number of controlling parameters (blend ratios, molecular weights and volume fractions) provide much richer phase diagrams than those of pure block terpolymers in three component systems.

Recently, we have reported that poly(isoprene-*block*-styrene-*block*-(2-vinyl pyridine)) (ISP) triblock terpolymer blends exhibited fantastic morphologies which cannot be found for simple ISP triblock terpolymers. They are a periodic undulated lamellar structure[33], rectangular-shaped cylinders[34] and cylindrical morphologies with nonconstant domain sizes and shapes.[35] Especially in binary blend of ISP triblock terpolymers with different chain lengths of two end-blocks, its oblong shape unit lattice of the cylindrical morphology has been found to be extremely large far beyond the size of individual domain, which was regarded as an approximant for a decagonal phase.[35]

Our purpose of the present work is to investigate the morphologies of the binary blends of ISP triblock terpolymer blends with asymmetric chain lengths of two end-blocks unlike our previous works in which the differences in chain lengths of the two-end blocks are almost the same.[35] Concretely in this work, the difference in molecular weights for I chains is 4 and that for P chains is 8, whereas the two ISP triblock terpolymers have similar total molecular weights and also similar molecular weights of central S component. The morphologies of the binary blends were carefully determined by TEM and SAXS measurements.

Experimental Sections

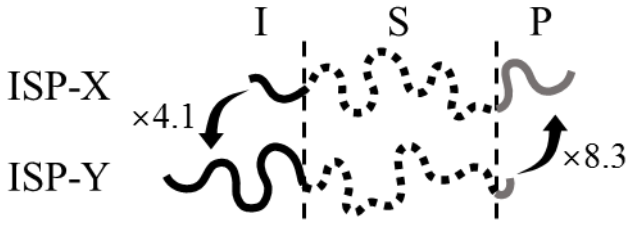

Figure 1. Schematic representation of the two ISP triblock terpolymers used in this study. Black, dashed and gray chains represent I, S and P, respectively. There are 4.1 and 8.3 times difference in chain lengths of I and P, respectively. The chain lengths of the two S chains are almost the same.

Table 1. Molecular characteristics of the poly(isoprene-*b*-styrene-*b*-(2-vinylpyridine)) (ISP) parent triblock terpolymers.

Sample	M_w (kg/mol) [a)]	M_n(I) : M_n(S) : M_n(P) (kg/mol) [b)]	$\varphi_I : \varphi_S : \varphi_P$ [b)]	M_w/M_n [c)]
ISP-X	223	25 : 150 : 50	0.12 : 0.67 : 0.21	1.02
ISP-Y	264	103 : 155 : 6	0.42 : 0.56 : 0.02	1.03

a) Determined by Osmometry

b) Determined by ^{1}H NMR spectroscopy using the densities of I, S and P at room temperature (ρ_I:0.926 g/cm^3, ρ_S:1.05 g/cm^3, ρ_P:1.14 g/cm^3).

c) Estimated from SEC chromatograms, whose elution volumes were calibrated with polystyrene standards.

Two kinds of poly(isoprene-*b*-styrene-*b*-(2-vinylpyridine)) linear triblock terpolymers, ISP-X and ISP-Y (Figure 1), were synthesized via sequential anionic polymerizations of I, S and P, followed by termination reactions with methanol. The details of syntheses were reported elsewhere.[12] Table 1 summarizes the characterization data of the two ISP triblock terpolymers prepared. The total molecular weights were determined by osmometry in benzene at 37°C with Osmomat 090 of Gonotec GmbH, and the molecular weights and the volume fractions of each component were estimated based on ^{1}H-NMR (Unity Inova500 of Varian Inc.) spectra in $CDCl_3$ using the densities I, S and P at room temperature (ρ_I:0.926 g/cm^3, ρ_S:1.05 g/cm^3, ρ_P:1.14 g/cm^3). The polydispersity indices, M_w/M_n were determined by size exclusion chromatography (SEC) which is composed of a set of pump, the DP-8020 (Shimadzu Co.), and a RI detector, RI-8020 (Shimadzu Co.) equipped with three polystyrene gel columns, TSK-gel G4000H_{HR} of Tosoh Co., using tetrahydrofuran (THF) as an eluent with 0.1 % addition of tetramethylethylenediamine (TMEDA). TMEDA was used to suppress adsorption of poly(2-vinylpyridine) on the polystyrene gel columns. The difference in molecular weights for I chains is 4.1, while that for P chains is 8.3.

The molecular characteristics of the binary mixtures of ISP-X and ISP-Y identified as Blend(X/Y) are listed in Table 2, where X is the molar ratio of ISP-X and Y is that of ISP-Y. The ratio of the volume fraction of two end components, φ_P/φ_I, is gradually changed as changing the blend ratio. The φ_P/φ_I is a good indicator to express the degree of asymmetry.[26]

Table 2. Molecular characteristics of blend samples in this study.

Sample	$\varphi_I : \varphi_S : \varphi_P$	φ_P / φ_I
Blend(9/1)	0.16 : 0.66 : 0.18	1.13
Blend(8/2)	0.20 : 0.64 : 0.16	0.82
Blend(7/3)	0.23 : 0.63 : 0.14	0.62
Blend(6/4)	0.26 : 0.62 : 0.12	0.47
Blend(5/5)	0.29 : 0.61 : 0.10	0.36
Blend(4/6)	0.32 : 0.60 : 0.08	0.27
Blend(3/7)	0.34 : 0.59 : 0.07	0.20
Blend(2/8)	0.37 : 0.58 : 0.05	0.14
Blend(1/9)	0.40 : 0.57 : 0.03	0.09

All sample films for the morphological observation were prepared by solvent casting from 3 wt% solution in THF, which is a common good solvent for all components. The solvent was slowly evaporated over 2 weeks in a petri dish of PTFE at room temperature to achieve an equilibrium state. Subsequently, the films were dried under vacuum at room temperature for one day, followed by thermal annealing at 150 °C for five days.

TEM and SAXS measurements were carried out to examine the morphologies. For TEM observation, several small pieces of the annealed films were embedded in an epoxy resin and cured for 9 hours at 60°C. The embedded samples were ultramictomed to a thickness of ca. 50 nm using a Leica Ultracut UCT microtome with a Diatome diamond knife at room temperature. The ultrathin sections were floated on water and then transferred onto a Cu 300 mesh grid, they were stained with

osmium tetroxide (OsO_4) vapor for 3h at 70 ºC and iodine (I_2) vapor for 2h at 50 ºC. OsO_4 gives a strong contrast for I component and I_2 selectively stains P component. By two-step staining with both the reagents, I component obtains the strongest contrast and P component earns the mid contrast, that is, dark, white and gray contrasts represent I, S and P phases, respectively. TEM experiments were performed with a JEM-1400 (JEOL Ltd.), operated at an accelerating voltage of 120 kV. SAXS experiments were conducted using beamline 6A at Photon Factory (Tsukuba, Japan) and BL 8S3 of Aichi Synchrotron Radiation Center (Aichi, Japan). The wavelength of the X-ray and the sample-to-detector distance at Photon Factory were 0.15 nm and 2519 mm, respectively. The instrument was calibrated using a silver behenate powder as a standard, and 2D SAXS patterns were recorded using a Pilatus 1M detector (pixel size = 172 μm). The wavelength of the X-ray and the sample-to-detector distance at Aichi Synchrotron Radiation Center were 0.15 nm and 3965 mm, respectively. Lead stearate was used as a standard to calibrate the instrument and 2D SAXS patterns were recorded on an automated imaging plate detector (R-AXIS IV ++, pixel size = 100 μm). All SAXS experiments were performed for small sample pieces cut from the annealed bulk films, where X-ray was irradiated from the direction parallel to film surface.

Results and Discussion

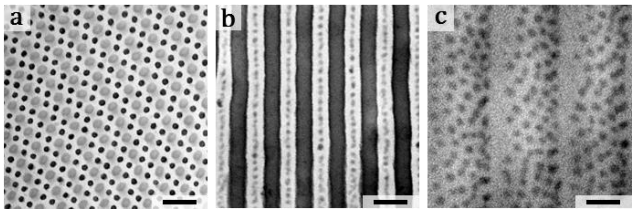

Figure 2. Representative TEM images of (a) ISP-X and (b) ISP-Y. (c) shows a image of ISP-Y stained only with I_2, which was taken perpendicular to lamellar surface with a shallow tilt angle. Scale bars represent 100 nm.

Figure 2 shows the periodic structures of the two parent ISP triblock terpolymers. The ISP-X in Figure 2(a) creates a hierarchical structure with double hexagonal symmetry, in which large hexagonal-packed P cylinders are surrounded by six thin I cylinders.[26] The ISP-Y forms a sphere-in-lamellae structure as shown in Figure 2(b), in which I and S phase exhibit alternative lamellae. The SAXS data of the ISP-X and ISP-Y shown in Figure S1 also reveal that ISP-X displays hexagonal symmetry and ISP-Y exhibits a lamellar structure, by the q/q_m ratios (q_m corresponds to the q value for the primary peak). The intercylinder and interlamella distances estimated from the q_m values are 83 nm and 104 nm, respectively, both of which agree reasonably well with the TEM results. Although P component has the largest electron density (I; 0.512 electron/cm^3, S; 0.565 electron/cm^3, P; 0.608 electron/cm^3), the diffraction peaks of the P spheres of ISP-Y were not detected in the SAXS data shown in Figure S1. This is probably because the volume fraction of the P component is not large

enough to detect the interference. Figure 2(c) reveals that the minor component P forms spherical domains packed hexagonally within a single layer at the center of S lamellae and the estimated diameter of the P spheres is about 11 nm.[19]

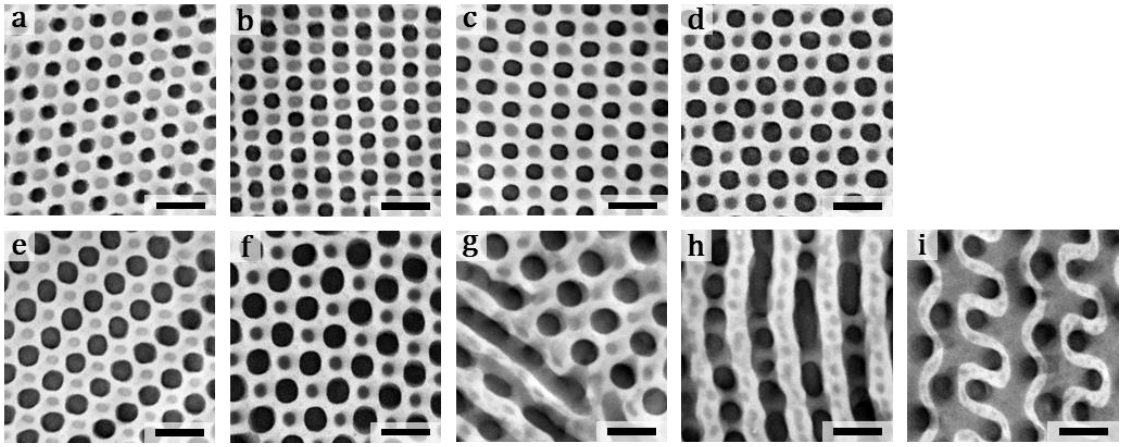

Figure 3. TEM images of the blend samples. (a) Blend(9/1), (b) Blend(8/2), (c) Blend(7/3), (d) Blend(6/4), (e) Blend(5/5), (f) Blend(4/6), (g) Blend(3/7), (h) Blend(2/8) and (i) Blend(1/9). Images from (a) to (f) show the cross sections of cylindrical morphologies. All scale bars represent 100 nm.

TEM images of all the blend samples listed in Table 2 are shown in Figure 3. Surprisingly, tetragonally packed cylinders, in which cylindrical I and P domains were co-arrayed tetragonally, were observed from Blend(9/1) to Blend(4/6) covering a wide range of φ_P/φ_I. Generally, co-arrayed tetragonal-packed cylinders are favored for ABC triblock terpolymers with symmetric composition with respect to A and C, i.e. φ_C/φ_A is close to unity. Namely A and C domains are forced to settle at

alternating locations equivalently within B matrix phase.[36] However, from the standpoint of filling space, hexagonal packing is more favorable than tetragonal one as is clearly realized in Figure 2(a) for an ABC triblock terpolymer with asymmetric end-block components.[37] That is, ABC triblock terpolymers with asymmetric end-block components are supposed to give hexagonally packed cylinders. Later we will try to give a more precise account of the characteristic tetragonal-packed cylinders.

At Blend(3/7), tetragonal cylinders and perforated lamella-like morphology were observed simultaneously, suggesting this blend is in a transit region. The Blend(2/8) shows a perforated lamella-like morphology covering the whole area, where a perforated layer of I and a complex layer of S and P are aligned alternately. At the same time, P spheres are distributed at the center of S phase. A TEM image of the Blend(1/9) has confirmed a double gyroid structure, in which I component conforms the double networks which are embedded in a complex matrix phase of S and P components. As for the matrix phase, P component could be spherical domains because its volume fraction is quite low, 0.03, and consequently the P spheres are periodically distributed over gyroid matrix phase of S.[35,38,39] We also found these morphologies in Blend(2/8) and Blend(1/9) interesting, but these structures lie outside the scope of this article, and hence we discuss them in supporting information (Figure S2 and S3).

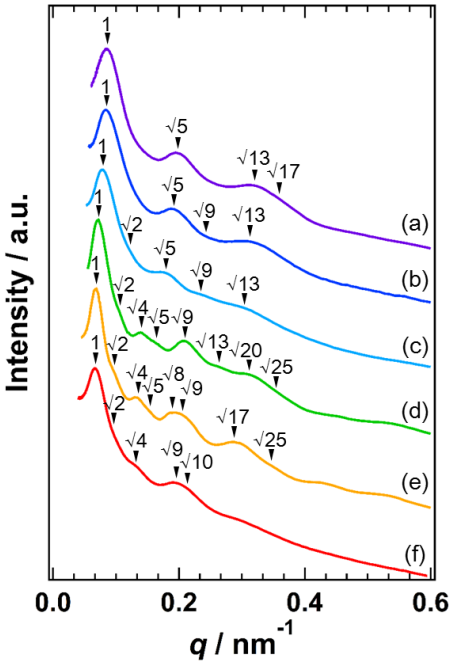

Figure 4. SAXS profiles of the blend samples in which tetragonal cylinders were observed from TEM. The SAXS profiles were obtained by azimuthally averaging 2D SAXS data. The sequence of peaks pointed out by inverted triangles is consistent with a tetragonal cylindrical arrangement. (a) Blend(9/1), (b) Blend(8/2), (c) Blend(7/3), (d) Blend(6/4), (e) Blend(5/5), (f) Blend(4/6).

It should be stressed on the fact that TEM images show local structures of bulk morphologies of block copolymers, while SAXS measurements provide structural information covering a wide area. Figure 4 displays the azimuthally integrated SAXS profiles for the blend samples possessing co-arrayed tetragonal-packed cylinders identified by TEM. All the SAXS patterns reveal the tetragonal manner from a series of diffraction peaks positioned in the order of q/q_m ratio, i.e. 1, √2, √4, √5, √8, √9 and so on. The domain distances between neighboring I cylinders or P cylinders estimated from

the first order peaks are summarized in Table 3. It is evident that the domain distance increases monotonically with increasing the blend ratio of ISP-Y.

Table 3. Summary of the domain distance (D) and the diameter of cylindrical domains calculated from Equation 7. Number of chains within a unit cell are estimated considering the molecular weight of the parent triblocks and the blend ratios, assuming that the number involved in Blend(9/1) is N.

	Blend(9/1)	Blend(8/2)	Blend(7/3)	Blend(6/4)	Blend(5/5)	Blend(4/6)
D [nm]	72	75	81	87	91	95
I cylinder [nm]	32	38	41	50	55	61
P cylinder [nm]	34	34	34	34	33	31
Number of chains in a unit cell	N	1.07N	1.22N	1.39N	1.49N	1.60N

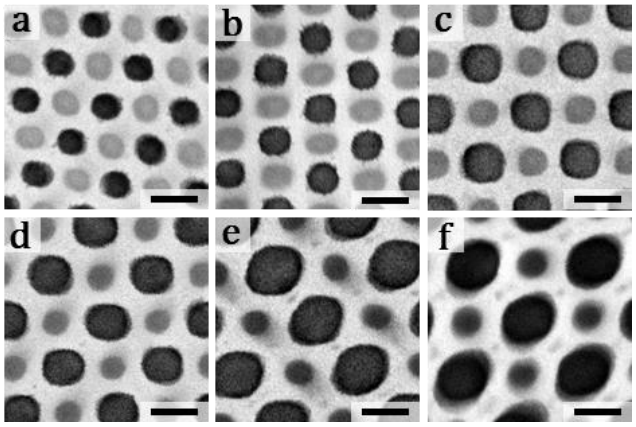

Figure 5. TEM images of the blend samples at high magnification. (a) Blend(9/1), (b) Blend(8/2), (c) Blend(7/3), (d) Blend(6/4), (e) Blend(5/5) and (f) Blend(4/6). All scale bars represent 50 nm.

The TEM images of the blend samples at high magnification are shown in Figure 5. These images clearly ensure tetragonal-packed cylinders and the increase in domain distance. It should be noted that we can easily find that the shape of the cross section of I cylinders is not just circle but rather close to square especially in Blend(7/3) and Blend(6/4), that is, the I domain is a rod rather than a cylinder in these blends. In our previous work, rods with 4-fold symmetry, which we called "rectangular-shaped cylinder" [34], were also found from binary blends of ISP triblock terpolymers with symmetric different chain length of the two end blocks. We concluded that the domains with non-constant mean curvature was formed due to weak localization of the junction point of two parent triblock terpolymers along the domain interface to release the conformational entropy losses of end blocks as well as centered S block. The I rods observed in this work are possibly generated by the same origin.

Here we can notice that the size of I domain is getting larger with increasing blend ratios of ISP-Y. This trend reflects the molecular design; as increasing the ratio of ISP-Y with long I chain, the volume fraction of I phase increases as is evident in Table 2. This will lead us further into a consideration of SAXS patterns shown in Figure 4. The difference in the domain size makes a large contribution to the scattering pattern. It is clearly confirmed that the relative peak positions and the relative intensities of the diffraction peaks have been changed systematically depending on the blend ratios, even though all samples indicate tetragonal-packed cylinders. Hence, we conducted the

calculation of scattering intensities of tetragonal-packed cylinders considering their domain sizes. For simplicity, the calculation was carried out based on the simplified structure factors, assuming both I and P domains possess cylindrical (circle) domains and the small P domains are neglected. See the Supporting Information for the details of the formulation.

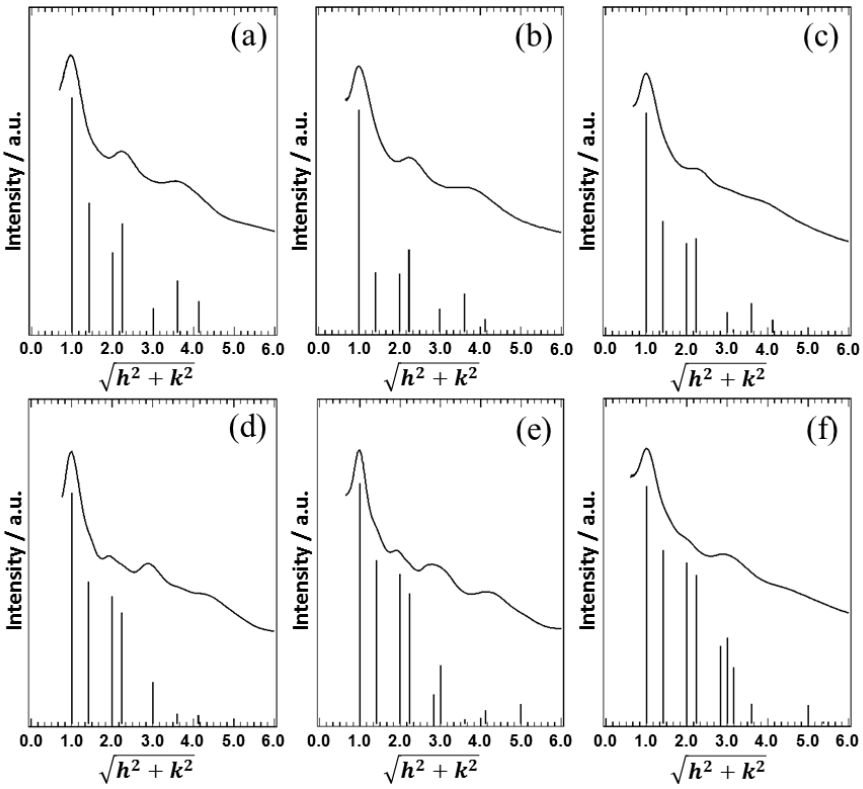

Figure 6. SAXS profiles of the blend samples and the intensity calculation results for each $\sqrt{h^2 + k^2}$, where *h* and *k* denote Miller index; (a) Blend(9/1), (b) Blend(8/2), (c) Blend(7/3), (d) Blend(6/4), (e) Blend(5/5), (f) Blend(4/6). The vertical bars express the relative intensities calculated from Equation 7 considering the sizes of I and P cylinders.

Figure 6 compares the calculated diffraction strengths associated with Equation 7 in Supporting Information and the experimental scattering profiles. As seen in Figure 6, the calculated intensities expressed with the vertical bars agree well with the SAXS data. Especially in Blend (5/5) in which many peaks were detected, the relative intensities and peak positions at (10), (11), (20), (21), (22) and (30) reflections are in good agreement with the experimental results. The diameters of cylindrical domains determined from the calculation are summarized in Table 3. Schematic illustrations at three X/Y compositions based on Table 3 are shown in Figure 7. From the values in Table 2 and 3, we have confirmed that the volume fractions evaluated from domain distance and domain size match well the exact volume fractions of the blend samples, as is clearly indicated in Figure S4. It is apparent from Table 3 that the diameter of I cylinder increases monotonically and that of P cylinder decreases very weakly as increasing the blend ratio of ISP-Y with long I chain and short P chain. These results can be understood by simply considering the number of chains within a unit cell increases from Blend(9/1) to (4/6). If the number of chains consisting in the 72×72 nm^2 unit cell of Blend(9/1) is taken to be N, 1.6N chains would be required to construct the 95×95 nm^2 unit cell of Blend(4/6), considering the total molecular weights of ISP-X and -Y and the blend ratios, and the estimated values are listed at the bottom in Table 3. This table tells the reason that the domain size of P spheres is almost constant even though the volume fraction of P component decreases, while that of I increases considerably with decreasing X/Y ratio. Thus the present results suggest that the domain

size directly depends on composition of samples even though all samples belong to the same space group (*p2mm* symmetry).

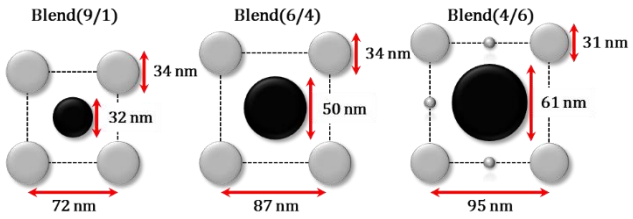

Figure 7. Schematic illustration of cross sections of tetragonally packed cylinders. The domain size and domain distance of each blend sample is based on the data in Table 3. Spherical small P domains located between P cylinders are added for Blend(4/6) as observed in Figure 5 and 8. Black and gray domains present I and P phases, respectively.

So far, we reported on the evident advantage of tetragonal-packed cylindrical or square-rod –like structures over others, even the case in which the size of I and P domains is highly asymmetric. There must be several reasons for this featured structure. One possible reason is the surface area difference. If Blend(6/4) is held up as an example, we notice S/P surface area for hexagonal arrangement is about $\sqrt{2}$ times larger than tetragonal one, this simply means hexagonal pattern is unfavorable. In reality, the present blend system chose tetragonal arrangement by sacrificing the conformational entropy of S chains. The small difference in two interaction parameters, i.e., $\chi_{S\text{-}P} > \chi_{S\text{-}I}$, probably help to realize this size asymmetric pattern.[26] The other possibility is the repulsive force

between I and P. Although these two components are not connected directly, in other words, no I/P interface exists, there might generate the long-range repulsive interaction between I and P, since these two components possess the highest interaction strength ($\chi_{S\text{-}P} \gg \chi_{S\text{-}P} \cong \chi_{S\text{-}I}$). This could cause geometrically alternative domain packing of I and P phases in matrix of S.

Moreover, we should not overlook the other specific features of the current morphologies. If we see the TEM images in Figure 5 (a)-(f) more carefully, quite small domains can be seen between I rods or P cylinders in Blend(5/5) and Blend(4/6). The small domains could not be observed in the other blend samples. Then we stained the blend samples with I_2 only to investigate the exact locations of the small P domains.

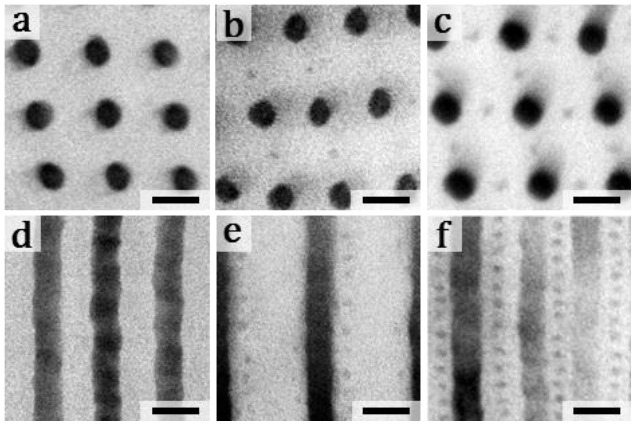

Figure 8. TEM images of blend samples stained with I_2; (a)(d) Blend(6/4), (b)(e) Blend(5/5) and (c)(g) Blend(4/6). Top images show the cross sectional view of P cylinders and bottom ones present their side views. The transverse views of Blend(6/4) and Blend(4/6) were obtained by the projection of [100] direction, while that of Blend(5/5) was observed from the [110] direction. For thin films (film

thickness < domain distance), the side view projections of cylindrical structures significantly depend on the observing direction. All scale bars represent 50 nm.

Figure 8 compares the TEM images of Blend(6/4), Blend(5/5) and Blend(4/6) stained with I_2. The upper images represent the cross sections of P cylinders while the bottom ones show their transverse views. P cylinders with tetragonal symmetry were simply found in Blend(6/4). On the other hand, small domains were observed in addition to P cylinders in Blend(5/5) and Blend(4/6). From the images for Blend(4/6), every large domain is surrounded by four small ones. Interestingly, Blend(5/5) presents that the P spheres do not align with regularity as shown in Figure 8(b) and (e). These results reveal that the number of the P spherical domains increases as increasing the ratio of ISP-Y with short P chain, resulting in an ordered array. The diameter of P spheres estimated from TEM is about 10 nm, which is close to the size of P sphere formed from neat ISP-Y. This implies that the P spheres are simply composed of the short P chains of ISP-Y.

For the moment, we shall discuss the asymmetric double tetragonal domain orientation with coexistent phase of spheres and cylinders. This unusual morphology was highly extended for binary blends of ABC triblock terpolymers with asymmetric different chain length in two end blocks.

The number of small P spheres increases gradually with the increase of fraction of ISP-Y as shown in Figure 8, resulting in the periodic sequence of P spheres aligning along P cylinders with

tetragonal symmetry. It is quite evident that short P chains of ISP-Y conform the P spheres because the size of P spheres is similar to that of neat ISP-Y as shown in Figure 2(b). That is, the excess short P chains can be expelled from P cylindrical domains, resulting in the formation of spherical domains. This phenomenon is analogous to coexisting phase for binary blends of AB diblock copolymers. Above a critical value of the length ratio of the constituent two diblock copolymers, the blend tends to choose two coexistent phases, one consists of two diblock copolymers and the other is composed of the short diblock chains only. The critical value of the length ratio was predicted to be about 5.[40,41]

In the present work, the chain length difference of I chains is not large enough to cause the separation of short and long chains, while it is large enough for P component, and hence short P chains are split into two domains so as to form the unusual structures with coexistent phase. At the same time, P spheres are located at the intermediate position between P cylinders because of the geometrical constraint of S chains. The P spheres can help to fill space well and admits the blend system stays still within the category of co-tetragonally packed domain structure. Consequently, in the present work, we have found tetragonal-packed cylinders at a wide range of φ_P/φ_I from 0.27 to 1.13.

Conclusion

In this study, we examined self-assembled structures from binary blends of ISP triblock terpolymers with asymmetric chain length of two end blocks. TEM and SAXS were used to investigate the morphological features. By blending the two ISP triblock terpolymers, nine blend from 9/1 to 1/9 were prepared, where co-arrayed tetragonal packed cylinders were observed covering wide range of volume fraction. SAXS analysis revealed that tetragonal cylinders are stable up to the Blend(4/6), in which $\varphi_{P/}\varphi_{I}$ is 0.27. This is unusual case for monodisperse ABC triblock terpolymers. What is interesting in this work is not only the fact that co-arrayed tetragonal cylinders were displayed on a wide range of volume fraction but that there are additional specific features: 1) I cylindrical domains was metamorphosed into rod domains in which the interface has non-constant mean curvature, 2) the cross-sectional area ratio of I domain/P domain is gradually increased with the volume fraction of each component and 3) spherical and cylindrical domains of P component coexist. The different chain length is definitely attributed to these features, and we expect that more interesting and complex morphologies will be developed from blend systems with chain length difference.

ASSOCIATED CONTENT

Supporting information:

The Supporting Information is available free of charge on the ACS Publication website.

TEM images and SAXS analysis (PDF)

AUTHOR INFORMATION

Corresponding Author:

*E-mail: yushu@apchem.nagoya-u.ac.jp

Notes:

The authors declare no competing financial interest.

Acknowledgement

This work was financially supported by Kakenhi (25248048), from MEXT; Y.M. is grateful for their support. Y.A. was financially supported by the Program for Leading Graduate Schools “Integrative Graduate Education and Research in Green Natural Sciences”, MEXT, Japan. The use of the synchrotron X-ray source was supported by Photon Factory, KEK, in Japan (No.2014G635) with the experimental assistance of Prof. N. Torikai. The SAXS experiments were conducted at the BL 8S3 of Aichi Synchrotron Radiation Center, Aichi Science & Technology Foundation, Aichi Japan (Proposal

No.201504085).

References

1. Bates, F. S.; Fredrickson, G. H. Block Copolymers – Designer Soft Materials. *Physics Today* **1999**, *52*, 32-38.

2. Abetz, V.; Simon, P. F. W. Phase Behaviour and Morphologies of Block Polymers. *Adv. Polym. Sci.* **2005**, *189*, 125–212.

3. Matsushita, Y. Studies on Equilibrium Structures of Complex Polymers in Condensed Systems. *J. Polym. Sci., Part B: Polym. Phys.* **2000**, *38*, 1645-1655.

4. Matsushita, Y.; Choshi, H.; Fujimoto, T.; Nagasawa, M. Preparation and Morphological Properties of a Triblock Copolymer of the ABC Type. *Macromolecules* **1980**, *13*, 1053−1058.

5. Richards, R. W.; Thomason, J. L. A small angle neutron scattering investigation of block copolymers of styrene and isoprene in the solid state. *Polymer* **1981**, *22*, 581−589.

6. Helfand, E.; Wasserman, Z. R. Block Copolymer Theory. 4. Narrow Interphase Approximation. *Macromolecules* **1976**, *9*, 879−888.

7. Ludwik, L. Theory of Microphase Separation in Block Copolymers. *Macromolecules* **1980**, *13*, 1602−1617.

8. Hasegawa, H.; Tanaka, H.; Yamasaki, K.; Hashimoto, T. Bicontinuous Microdomain Morphology of Block Copolymers. 1. Tetrapod-Network Structure of Polystyrene-Polyisoprene Diblock Polymers. *Macromolecules* **1987**, *20*, 1651-1662.

9. Bates, F. S.; Schulz, M. F.; Khandpur, A. K.; Forster, S.; Rosedale, J. H. Fluctuation, Conformational Asymmetry and Block Copolymer Phase Behaviour. *Faraday Discuss*. **1994**, *98*, 7-18.

10. Khandpur, A. K.; Forster, S.; Bates, F.S.; Hamley, I. W.; Ryan, A. J.; Bras, W.; Almdal, K.; Mortensen, K. Polyisoprene-Polystyrene Diblock Copolymer Phase Diagram near the Order-Disorder Transition. *Macromolecules* **1995**, *28*, 8796-8806.

11. Matsen, M. W. Effect of Architecture on the Phase Behavior of AB-Type Block Copolymer Melts. *Macromolecules* **2012**, *45*, 2162-2165.

12. Mogi, Y.; Kotsuji, H.; Kaneko, Y.; Mori, K.; Matsushita, Y.; Noda, I. Preparation and Morphology of Triblock Copolymers of the ABC Type. *Macromolecules* **1992**, *25*, 5408-5411.

13. Suzuki, J; Seki, M.; Matsushita, Y. The tricontinuous double-gyroid structure from a three-component polymer system. *J. Chem. Phys.* **2000**, *112*, 4862-4868.

14. Gido, S. P.; Schwark, D. W.; Thomas, E. L. Observation of a Non-Constant Mean Curvature Interface in an ABC Triblock Copolymer. *Macromolecules* **1993**, *26*, 2636-2640.

15. Matsushita, Y.; Tamura, M.; Noda, I. Tricontinuous Double-Diamond Structure Formed by a Styrene-Isoprene-2-Vinylpyridine Triblock Copolymer. *Macromolecules* **1994**, *27*, 3680-3682.

16. Ishige, R.; Higuchi, T.; Jiang, X.; Mita, K.; Ogawa, H.; Yokoyama, H.; Takahara, A.; Jinnai, H. Structural Analysis of Microphase Separated Interface in an ABC-Type Triblock Terpolymer by Combining Methods of Synchrotron-Radiation Grazing Incidence Small-Angle X-ray Scattering and Electron Microtomography. *Macromolecules* **2015**, *48*, 2697-2705.

17. Breiner, U.; Krappe, U.; Stadler, R. Evolution of the "knitting pattern" morphology in ABC triblock copolymers. *Macromol. Rapid Commun.* **1996**, *17*, 567-575.

18. Epps, T. H. III.; Cochran, E. W.; Hardy, C. M.; Bailey, T. S.; Waletzko, R. S.; Bates, F. S. Network Phase in ABC Triblock Copolymers. *Macromolecules* **2004**, *37*, 7085-7088.

19. Zhang, W.; Wang, Z.-G. Morphology of ABC Triblock Copolymers. *Macromolecules* **1995**, *28*, 7215-7223.

20. Tang, P.; Qiu, F.; Zhang, H.; Yang, Y. Morphology and phase diagram of complex block copolymers: ABC linear triblock copolymers. *Phys Rev. E* **2004**, *69*, 031803.

21. Qin, J.; Bates, F. S.; Morse, D. C. Phase Behavior of Nonfrustrated ABC Triblock Copolymers: Weak and Intermediate Segregation. *Macromolecules* **2010**, *43*, 5128-5136.

22. Liu, M.; Li, W.; Qiu, F.; Shi, A.-C. Theoretical Study of Phase Behavior of Frustrated ABC Linear Triblock Copolymers. *Macromolecules* **2012**, *45*, 9522-9530.

23. Tureau, M. S.; Rong, L.; Hsiao, B. S.; Epps, T. H. III. Phase Behavior of Neat Triblock Copolymers and Copolymer/Homopolymer Blends Near Network Phase Windows. *Macromolecules* **2010**, *43*, 9039-9048.

24. Suzuki, J.; Furuya, M.; Iinuma, M.; Takano, A.; Matsushita, Y. Morphology of ABC Triblock Copolymer/Homopolymer Blend Systems. *J. Polym. Sci., Part B: Polym. Phys.* **2002**, *40*, 1135-1141.

25. Sugiyama, M.; Shefelbine, T. A.; Vigild, M. E.; Bates, F. S. Phase Behavior of an ABC Triblock Copolymer Blended with A and C Homopolymers. *J. Phys. Chem. B* **2001**, *105*, 12448-12460.

26. Izumi, Y.; Yamada, M.; Takano, A.; Matsushita, Y. A New Periodic Pattern with Five-Neighbored Domain Packing from ABC Triblock Terpolymer/B Homopolymer Blend. *J. Polym. Sci., Part B: Polym. Phys* **2015**, *53*, 907-911.

Note: In this work, it has been confirmed that ISP/S homopolymer blend system show asymmetric phase diagram. That is, ISP/S blends possess double hexagonal-packed cylindrical structure composed of large P cylinders surrounded by six thin I cylinders covering wide range of $\varphi_{P/}\ \varphi_{I}$, while $\varphi_{P/}\ \varphi_{I}$ region for double hexagonal cylinders with thick I cylinders surrounded by six thin P cylinders is narrow. This asymmetric phase diagram could be originated from the difference in χ values between S-I and S-P ($\chi_{S\text{-}P} > \chi_{S\text{-}I}$).

27. Dotera, T. Tricontinuous Cubic Structures in ABC/A/C Copolymer and Homopolymer Blends. *Phys. Rev. Lett.* **2002**, *89*, 205502.

28. Goldacker, T.; Abetz, V. Core-Shell Cylinders and Core-Shell Gyroid Morphologies via Blending of Lamellar ABC Triblock and BC Diblock Copolymers. *Macromolecules* **1999**, *32*, 5165-5167.

29. Birshtein, T. M.; Polotsky, A. A.; Abetz, V. Mixed Supercrystalline Structures in Mixtures of ABC Triblock and ab(bc) Diblock Copolymers, 3ª Lamellar and Cylindrical Structures in Bicomponent Mixtures. *Macromol Theory Sumul* **2001**. *10*. 700-718.

30. Goldacker, T.; Abetz, V.; Stadler, R.; Erukhimovich, I.; Leibler, L. Non-centrosymmetric superlattices in block copolymer blends. *Nature* **1999**, *398*, 137-139.

31. Wickham, R. A.; Shi, A.-C. Noncentrosymmetric Lamellar Phase in Blends of ABC Triblock and ac Diblock Copolymers. *Macromolecules* **2001**, *34*, 6487-6494.

32. Abetz, V.; Goldacker, T. Formation of superlattices via blending of block copolymers. *Macromol. Rapid Commun.* **2000**, *21*, 16-34.

33. Matsushita, Y.; Suzuki, J.; Izumi, K.; Matsuoka, K.; Takahashi, S.; Aoyama, Y.; Mihira, T.; Takano, A. Formation of undulated lamellar structure from ABC block terpolymer blends with different chain lengths. *J. Chem. Phys* **2010**, *133*, 194901.

34. Asai, Y.; Yamada, K.; Yamada, M.; Takano, A.; Matsushita, Y. Formation of Tetragonally-Packed Rectangular Cylinders from ABC Block Terpolymer Blends. *ACS Macro Lett.* **2014**, *3*, 166-169.

35. Asai, Y.; Takano, A.; Matsushita, Y. Creation of Cylindrical Morphologies with Extremely Large Oblong Unit Lattices from ABC Block Terpolymer Blends. *Macromolecules* **2015**, *48*, 1538-1542.

36. Matsen, M. W. Gyroid versus double-diamond in ABC triblock copolymer melts. *J. Chem. Phys.* **1998**, *108*, 785-796.

37. Tyler, C. A.; Qin, A.; Bates, F. S.; Morse, D. C. SCFT Study of Nonfrustrated ABC Triblock Copolymer Melt. *Macromolecules* **2007**, *40*, 4654-4668.

38. Dotera, T.; Kimoto, M.; Matsuzawa, J. Hard spheres on the gyroid surface. *Interface Focus* **2012**, 2, 575-581.

39. Kirkensgaard, J. J. K. Kaleidoscopic tilings, networks and hierarchical structures in blends of 3-miktoarm star terpolymers. *Interface Focus* **2012**. 2. 602-607.

40. Matsen, M.W. Immiscibility of large and small symmetric diblock copolymers. *J. Chem. Phys.* **1995**, *103*, 3268-3271.

41. Yamaguchi, D.; Hashimoto, T. A Phase Diagram for the Binary Blends of Nearly Symmetric Diblock Copolymers. 1. Parameter Space of Molecular Weight Ratio and Blend Composition. *Macromolecules* **2001**, *34*, 6495-6505.

for Table of Contents use only

Asymmetric Double Tetragonal Domain Orientation from ABC Triblock Terpolymer Blends with Chain Length Difference

Yusuke Asai, Atsushi Takano, Yushu Matsushita*